Recyclable deep eutectic solvent for the production of cationic nanocelluloses

Panpan Li,[a] *Juho Antti Sirviö,*[a] *Bright Asante,*[b] *and Henrikki Liimatainen*,*[a]

[a] Fibre and Particle Engineering Research Unit, University of Oulu, P.O. Box 4300, FI-90014 Finland

[b] Wood Materials Science, University of Eastern Finland, P. O. Box 111, FI-80101, Finland

Henrikki Liimatainen; Henrikki.Liimatainen@oulu.fi (corresponding author)

Panpan Li; Panpan.Li@oulu.fi

Juho Antti Sirviö; Juho.Sirvio@oulu.fi

Bright Asante; basante1991@gmail.com

***Corresponding Author**

E-mail: Henrikki.Liimatainen@oulu.fi

Tel.: +358 505659711 Fax: +358 8344084

Highlights

- A new deep eutectic solvent was developed to produce cationic cellulose
- Both cationic cellulose nanofibrils and cellulose nanocrystals can be produced
- This deep eutectic solvent can be re-used over 5 times at stable efficiency
- No additional chemical is needed for the reproduction of cationic cellulose

Graphical abstract

ABSTRACT:

Deep eutectic solvents (DESs) are potential green systems that can be used as reagents, extraction agents and reaction media. DESs are often biodegradable, easy to prepare and have low toxicity. In this work, a recyclable DES formed from aminoguanidine hydrochloride and glycerol (AhG) was used as a reaction medium and reagent (aminoguanidine hydrochloride) for the production of cationic nanocelluloses. Under mild conditions (i.e., a reaction time of 10 min at 70°C), dialdehyde celluloses (DACs) with two different aldehyde contents (2.18 and 3.79 mmol g^{-1}) were cationized by AhG DES to form cationic dialdehyde celluloses (CDACs). Both CDACs achieved a similar high charge density of approximately 1.1 mmol g^{-1}. At 80°C (for 10 min), a very high cationic charge density of 2.48 mmol g^{-1} was obtained. The recyclability of AhG DES was demonstrated by reusing it five times without decreasing the reaction efficiency. In particular, due to the low consumption of amoniguanidine hydrochloride, high recycling efficiency could be achieved without the use of any additional chemicals. The cationized celluloses, CDACs, were further mechanically disintegrated to obtain cationic nanocelluloses. According to the initial aldehyde content of DACs, the morphology of the nanocellulose could be tailored to produce highly cationic cellulose nanofibrils (CNFs) or cellulose nanocrystals (CNCs). Transmission electron microscopy confirmed that individual CNFs and CNCs with an average width of 4.6 ± 1.1 nm and 5.7 ± 1.3 nm, respectively, were obtained. Thus, the results presented here indicate that the AhG DES is a promising green and recyclable way of producing cationized CNFs and CNCs.

KEYWORDS: Cationization, Nanocellulose, Recycle, Deep eutectic solvents.

1. INTRODUCTION

Selection of the appropriate reaction medium is critical to many chemical processes, and c.a. 80% of all consumed chemicals are used as solvents for different purposes.(Cruz, Jordão, & Branco, 2017) Traditional solvents are usually prepared from non-renewable and toxic petrochemical derivatives,(Gu & Jérôme, 2010) and they are often highly volatile, flammable and problematic for the environment.(Alonso et al., 2016) As a consequence of the depletion of oil resources and increasing environmental awareness, there has been growing interest in exploring alternative solvents such as water,(C.-J. Li & Chen, 2006) fluorinated compounds,(Khaksar, 2015) and ionic liquids (ILs)(Imperato, König, & Chiappe, 2007) in the past decade. Although promising results have been reported, obvious limitations (such as high cost and requirement for high purity of ILs) still restrict their practical use in many cases. Therefore, new green and easily available solvents are in high demand. (Q. Zhang, De Oliveira Vigier, Royer, & Jérôme, 2012)

Currently, deep eutectic solvents (DESs) are of particular interest. The complexation of a hydrogen bond acceptor (HBA, which is typically a halide salt of quaternary ammonium) with a hydrogen bond donor (HBD, e.g., urea and glycerol) results in the formation of an eutectic mixture with a relatively low melting point, and this is how DESs are usually produced. (Paiva et al., 2014; J. A. Sirviö, Visanko, & Liimatainen, 2015; Smith, Abbott, & Ryder, 2014; Wagle, Zhao, & Baker, 2014; Q. Zhang et al., 2012) DES candidates are abundant, and they can be produced from inexpensive, biodegradable and recyclable ingredients.(Ilgen et al., 2009; Singh, Lobo, & Shankarling, 2011; J. A. Sirviö, Visanko, Ukkola, & Liimatainen, 2018) Similar to ILs, DESs exhibit good solvent capacity and have a low vapor pressure that limits VOC emissions.(J. A.

Sirviö, Visanko, et al., 2015; J. A. Sirviö, Visanko, & Liimatainen, 2016; Smith et al., 2014) However, it is much easier to prepare DESs (by straightforward mixing and heating), and they are less sensitive to impurities and usually cheaper to prepare than ILs.(Wang et al., 2016) These unique properties make DESs promising green solvents and chemicals for sustainable biomaterial production processes.

Cellulose is known as the most abundant natural biopolymer on earth. In addition, renewability, biodegradability, and low toxicity are all inherent green characteristics of cellulose.(Credou & Berthelot, 2014; Schenzel, Hufendiek, Barner-Kowollik, & Meier, 2014) Nanocelluloses, which are described as nano-structured celluloses and are often referred to as elongated cellulose nanofibrils (CNFs) or rigid cellulose nanocrystals (CNCs), have been considered as future biomaterials in recent years.(Moon, Martini, Nairn, Simonsen, & Youngblood, 2011) Depending on the raw materials and production methods, CNFs are mostly 3−100 nm in width and several micrometers in length,(Klemm et al., 2011) whereas CNCs have a similar diameter but are shorter and have a more rod-like crystalline structure. Nanocelluloses possess certain inherent chemical characteristics (e.g., three reactive hydroxyl groups in each repeating unit) of celluloses, are lightweight,(Mohieldin, Zainudin, Paridah, & Ainun, 2011) and have high mechanical strength(Oksman, Mathew, Bondeson, & Kvien, 2006) and good thermal stability.(P. Li, Sirviö, Haapala, & Liimatainen, 2017) These favorable properties make nanocelluloses a promising resource in advanced applications such as UV-absorbing fillers for nanocomposites,(J. A. Sirviö, Visanko, Heiskanen, & Liimatainen, 2016) substrates for organic solar cells,(Zhou et al., 2014) agents for mineral flotation(O. Laitinen et al., 2016; Ossi Laitinen et al., 2014) and stabilizers of oil-water emulsions.(Ojala, Sirviö, & Liimatainen, 2016)

Typically, CNFs are produced through a mechanical nanofibrillation procedure (e.g., refining, grinding, and homogenization), which requires a significant amount of energy due to the highly ordered hydrogen bond network of cellulose.(Baati, Magnin, & Boufi, 2017; J. A. Sirviö, Hasa, et al., 2015) Nevertheless, the high energy consumption can be reduced with the use of chemically modified,(H. Liimatainen, Visanko, Sirviö, Hormi, & Niinimaki, 2012; Henrikki Liimatainen, Suopajärvi, Sirviö, Hormi, & Niinimäki, 2014; Saito, Nishiyama, Putaux, Vignon, & Isogai, 2006; Selkälä, Sirviö, Lorite, & Liimatainen, 2016) enzyme-assisted,(Henriksson, Henriksson, Berglund, & Lindström, 2007; Shahid, Mohammad, Chen, Tang, & Xing, 2016) or solvent-disintegrated(P. Li et al., 2017; J. A. Sirviö, Visanko, et al., 2015) pretreatment approaches.(Siró & Plackett, 2010a) Unlike CNFs, CNCs can be conventionally fabricated by simple acidic (e.g., sulfuric,(Bondeson, Mathew, & Oksman, 2006) hydrochloric,(Yu et al., 2013) or phosphoric acid(Camarero Espinosa, Kuhnt, Foster, & Weder, 2013)) hydrolysis of the amorphous regions of cellulose, which releases the hard crystalline parts of cellulose. However, there are noticeable limitations to acidic hydrolysis methods, such as material corrosion, sensitive reaction conditions, low production yield,(Corrêa, de Morais Teixeira, Pessan, & Mattoso, 2010; Lu et al., 2016) and fiber aggregation.(Araki, Wada, Kuga, & Okano, 1998) Therefore, oxidation-based methods such as TEMPO-,(Qin, Tong, Chin, & Zhou, 2011) persulfate(Leung et al., 2011; K. Zhang et al., 2016) and periodate oxidation(Visanko et al., 2014) have been developed not only to compensate for the shortcomings of acidic hydrolysis methods, but also to expand functionalized CNC production.(Montanari, Roumani, Heux, & Vignon, 2005; J. A. Sirviö, Visanko, Heiskanen, et al., 2016; Visanko et al., 2014)

The introduction of cationic groups on cellulose fibers can enhance nanocellulose production and prevent the aggregation of nanocelluloses due to electrostatic repulsion.(Visanko et al., 2014) In

addition, introduction of cationically charged groups combined with alkyl chains, such as aminated structures, to the hydrophilic backbone of cellulose can result in the formation of amphiphilic nanocelluloses, which have potential for use as a stabilizer in oil-water emulsions,(Visanko et al., 2014) flocculation agent in dewatering,(Suopajärvi, Sirviö, & Liimatainen, 2017a) or a colloid aggregation agent.(Henrikki Liimatainen et al., 2014) Previously, cationized nanocelluloses have been synthesized in epoxypropyltrimethylammonium chloride,(Hasani, Cranston, Westman, & Gray, 2008) imidazolium,(Eyley & Thielemans, 2011) pyridinium(Jasmani, Eyley, Wallbridge, & Thielemans, 2013) and water.(Hua et al., 2014; J. A. Sirviö et al., 2014a; J. Sirviö, Honka, Liimatainen, Niinimäki, & Hormi, 2011; Yang & van de Ven, 2016)

DESs have been used as alternative green routes to produce both non-derivatized (Ossi Laitinen, Suopajärvi, Österberg, & Liimatainen, 2017; P. Li et al., 2017; J. A. Sirviö, Visanko, et al., 2015; Suopajärvi, Sirviö, & Liimatainen, 2017b) and anionic(Ossi Laitinen, Ojala, Sirviö, & Liimatainen, 2017; Selkälä et al., 2016; J. A. Sirviö, Visanko, & Liimatainen, 2016; J. A. Sirviö & Visanko, 2017) nanocelluloses, but there was very few reports about its use for the fabrication of cationized nanocelluloses.(J. A. Sirviö, n.d.) Thus, to the best of our knowledge, this is the first time that a recyclable and effective DES was developed to produce cationic nanocelluloses. In this work, a DES produced using aminoguanidine hydrochloride and glycerol (AhG) was used as a reaction medium and reagent (aminoguanidine hydrochloride) for cationization of dialdehyde cellulose (DAC). Birch cellulose was first oxidized to DAC using recyclable sodium periodate(Jin, Li, Xu, & Sun, 2015; Henrikki Liimatainen, Sirviö, Pajari, Hormi, & Niinimäki, 2013; J. Zhang, Jiang, Dang, Elder, & Ragauskas, 2008) and then cationized by the AhG DES to produce cationic dialdehyde celluloses (CDACs) under different temperatures and reaction times. The CDACs that were synthesized at 70°C for 10 min were selected and further mechanically nanofibrillated to

obtain cationized nanocelluloses. The recyclability and yield of the DES were analyzed. The charge densities of CDACs were investigated by polyelectrolytic titration, and attenuated total reflection infrared (ATR-IR) spectroscopy was used for the chemical characterization of celluloses. Cationized nanocelluloses were characterized by transmission electron microscopy (TEM).

2. Materials and methods

2.1 Materials

Bleached kraft birch (*Betula pendula*) pulp sheets were used as cellulose raw material after they were disintegrated in deionized water. The properties of the pulp have been determined in a previous study.(Henrikki Liimatainen, Sirviö, Haapala, Hormi, & Niinimäki, 2011) Lithium chloride (99%) and sodium periodate (>99%) were obtained from Sigma Aldrich (Germany) to produce dialdehyde cellulose. Ethanol (96%) and glycerol (97%) (VWR, France) and aminoguanidine hydrochloride (>98%) (Tokyo Chemicals Industry, Japan) were used for the cationization of dialdehyde cellulose. Sodium polyethylene sulfonate (PES-Na) from BTG (UK) was used as a polyelectrolyte to determine the cationic charge. Uranyl acetate dihydrate (98%) was from Polysciences (Germany). Polylysine solution (0.01%) was from Sigma Aldrich (Germany). Deionized water was also used throughout the study.

2.2 Synthesis of CDACs in the AhG DES

DAC was obtained from birch pulp by a slightly modified version of the sodium periodate oxidation method reported previously.(Dash, Elder, & Ragauskas, 2012; Sirvio, Hyvakko, Liimatainen, Niinimaki, & Hormi, 2011) Briefly, 10 g (abs.) of birch pulp was diluted with 1000

111 g of deionized water, and the suspension was heated to a final temperature of 55°C or 75°C in an
112 oil-bath system. Following this, 18 g of lithium chloride (LiCl) and 8.2 g of sodium periodate
113 ($NaIO_4$) were added and left to react with cellulose for 3 h at their respective temperatures. The
114 mixed reaction suspensions were fully covered with an aluminum foil to avoid light-induced
115 decomposition of periodate. The products were filtered, washed with 1000 ml of a 50:50
116 ethanol:water solution, mixed in 500 ml ethanol twice for 15 min, and filtrated. According to the
117 reaction temperature (55°C or 75°C), the DAC products were labeled as DAC55 or DAC75.

118 The AhG DES was prepared by mixing 75 g aminoguanidine hydrochloride and 125 g glycerol
119 in a molar ratio of 1:2 in a Scott bottle. The mixture was preheated at 90°C in an oil bath to obtain
120 a clear liquid, and then adjusted to the desired reaction temperatures (70, 80, 90, and 100°C).
121 Following this, 10 g (abs.) DAC55 or DAC75 was added into the DES, which was stirred
122 continuously with a magnetic bar for a set of reaction times (5, 10, 15, 30 and 60 min) at the desired
123 temperatures. The reaction bottle was removed from the oil-bath system and 250 ml of ethanol
124 was added. The product suspension was filtrated and washed twice with 500 ml of ethanol. The
125 filtrate (DES-ethanol solution) was collected for the next cationization cycle. The yield of CDACs
126 was recorded.

127 *2.3 ATR-IR*

128 The FTIR spectra of birch cellulose, DAC75 and CDAC75 (synthesized from the original DES
129 at 70°C for 10 min) were recorded with a Bruker IR spectrometer (Bruker Tensor II FTIR
130 Spectrometer, USA) equipped with an attenuated total reflection (ATR) accessory. The samples
131 were prepared by pressing 0.2 g (abs.) dried sample into a pellet.

132 *2.4 Fabrication of cationized nanocelluloses*

CDAC55 and CDAC75 synthesized with the AhG DES at 70°C for 10 min were selected for nanofibrillation. Cationized nanocelluloses were produced by mechanical disintegration of 1% CDAC55 or CDAC75 solution with a microfluidizer (Microfluidics M-110EH-30, USA). Both CDAC55 and CDAC75 were treated similarly: they were first stirred with a magnetic bar for 10 min and then passed through a pair of chambers (400 and 200 μm) twice in a microfluidizer under a pressure of 1000 bars.

2.5 TEM

The morphological features of the cationized nanocelluloses were observed with the help of a Tecnai G2 Spirit transmission electron microscope (FEI Europe, Eindhoven, The Netherlands). Nanocellulose samples were diluted with deionized water into a 0.01% solution (w/w), and a tiny droplet (7 μL) of polylysine used as adhesive of nanocellulose sample(Marsich et al., 2012) was first dosed on the top of a Butvar and carbon-coated copper grid and left for 1 min. Excess polylysine was wiped off with a filter paper. Similarly, 7 μL of the nanocellulose sample solution was then dropped, stayed and removed from the grid. Finally, a drop of negative staining agent, uranyl acetate (2% [w/v]), was applied using the same procedure. The stained samples were dried at room temperature and were later analyzed at 100 kV under standard conditions. Images were taken with a Quemesa CCD camera. The width of individual nanofibrils or nanocrystals was measured using the iTEM image analysis software (Olympus Soft Imaging Solutions GMBH, Munster, Germany). The data obtained are presented as the mean and standard errors.

2.6 Determination of cationic charge

The cationic charge density of CDACs was determined using the polyelectrolyte titration method with a particle charge detector (BTG Mütek PCD-03, Germany). The CDACs were diluted

with deionized water into a 0.01% solution and stirred with a magnetic stirrer at room temperature for 30 min. Then, 10 ml of well-dispersed CDAC suspension was titrated with the sodium polyethylene sulfonate (PES-Na) polyelectrolyte. The charge density was calculated based on the consumption of PES-Na. The results are the average of two trials with minor difference.

2.7 Recycling of the AhG DES

The collected filtrate containing the AhG DES and ethanol from the cationization reaction was distilled under reduced pressure at 50°C using a rotatory evaporator (Büchi rotavapor R114, Switzerland) in a water bath. The recycled DES was reheated to 70°C and reused in the cationization of DACs (10-min reaction), in a similar manner as described earlier. The recycling was repeated five times without the use of any additional chemicals.

2.8 The yield calculation

The yields of CDAC55 and CDAC75 were calculated by the measurement of mass differences, before and after chemical treatment. However, the yield of recycled DES was calculated by the measurement of mass differences, compared with original DES.

2.9 Thermogravimetric Analysis

Thermogravimetric analysis (TGA) of original AhG DES was carried out by a thermal analyzer (Netzsch STA 449F3 apparatus) under air atmospheres; the air flow (dynamic air), at a constant rate of 60 mL min^{-1}. Approximate 20 mg of well mixed AhG DES was added into an aluminum pan and was heated from 20 to 650 °C with a heating rate at 10 °C min^{-1}. The decomposition temperature (Td) was taken when the temperature at the onset point of the weight loss in the TGA curve was obtained.

2.10 X-ray diffraction

The crystalline structures of the CDAC55 and CDAC75 were investigated using wide-angle X-ray diffraction. Measurements were conducted on a Rigaku SmartLab 9 kW rotating anode diffractometer (Japan) equipped with a Cu Kα radiation source (λ = 0.1542 nm) at 45kV, 200mA. Specimens were prepared by pressing tablets with a thickness of 1 mm after freeze-drying the samples. Scans were taken over a 2θ (Bragg angle) range from 5° to 50° at a scanning speed of 2° s min^{-1} using a step of 0.05°. The degree of the peak intensity of the main crystalline plane (200) diffraction (I_{200}) was located at 22.5°. The peak intensity associated with the amorphous fraction of cellulose (I_{am}) was observed at 18.0°. Crystallinity index (CrI) values were calculated according to the empirical Segal method. (Segal, Creely, A. E. Martin, & Conrad, 2016)

$$\mathrm{CrI} = \left(\frac{\mathrm{I_{200}} - \mathrm{I_{am}}}{\mathrm{I_{200}}}\right) \times 100\%$$

3. Results and discussion

The AhG DES was prepared by aminoguanidine hydrochloride and glycerol in a molar ratio of 1:2. The cationization of DAC was conducted in AhG DES, in which glycerol was applied as an HBD to help with the formation of an efficient and continuously derivable DES from aminoguanidine hydrochloride.(J. A. Sirviö, Visanko, et al., 2015; Smith et al., 2014; Wagle et al., 2014; W. Zhang, Barone, & Renneckar, 2015) Glycerol is a well-known natural polyol that is often obtained as a by-product of the transesterification of a triglyceride in natural fatty acid production.(Wolfson, Dlugy, & Shotland, 2007) Glycerol has the combined advantages of water (which is renewable, inexpensive and abundant) and ILs (which has a high boiling point and low

197 vapor pressure),(Gu & Jérôme, 2010) which make it an alternative green medium for catalytic and
198 non-catalytic reactions.(Kong et al., 2016; Wolfson et al., 2007) In addition to pure glycerol,
199 glycerol-based solvent systems have also been reported as a reaction medium for organic
200 synthesis,(García, García-Marín, & Pires, 2014) as a co-solvent for biotransformation,(Hernáiz,
201 Alcántara, García, & Sinisterra, 2010; Wolfson, Dlugy, Tavor, Blumenfeld, & Shotland, 2006) as
202 a dual solvent-reagent system for hydrogenation reaction,(Cravotto et al., 2011; Díaz-Álvarez,
203 Crochet, & Cadierno, 2011) and as an HBD for DES formation.(Abbott et al., 2011; Abbott, Cullis,
204 Gibson, Harris, & Raven, 2007; Zhao & Baker, 2013) In the literature, similar DESs formed by
205 choline chloride–glycerol have also been studied and applied as a medium for the desulfurization
206 of fuel and the absorption of CO_2 and SO_2.(Abbott et al., 2011; García et al., 2014) However, in
207 the present case, the AhG DES was used as a derivatizing solvent for cellulose cationization.

208

209 *3.1 Cationization of DAC in AhG DES*

210 The reaction between DAC and aminoguanidine hydrochloride resulted in the formation of a
211 stable imine bond, and thus could be used to introduce cationic groups to DAC (Figure 1).(J. A.
212 Sirviö et al., 2014b; J. Sirviö et al., 2011) Here, DAC55 and DAC75 (which have an aldehyde
213 content of 2.18 and 3.79 mmol g^{-1}, respectively, as determined previously(Sirvio et al., 2011))
214 were successfully further cationized (CDAC55 and CDAC75) using a set of reaction times (5, 10,
215 15, 30 and 60 min) and temperatures (70, 80, 90 and 100°C).

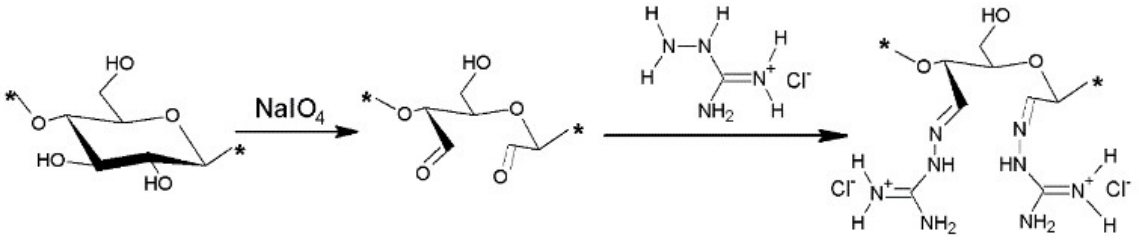

Figure 1. Cationization of cellulose using sequential periodate oxidation and imidization with aminoguanidine hydrochloride.

The original AhG DES that was formed by the mixing of aminoguanidine hydrochloride and glycerol became a clear and colorless liquid at 90°C. The heating temperature was crucial to DES formation; i.e., a clear solution was obtained rapidly at 90 and 100°C, but a more turbid solution was obtained at 70 and 80°C. Therefore, the DES was first heated to 90°C, and then the temperature was adjusted to the desired reaction temperature. The addition of DAC into DES (at a mass ratio of 1:20) resulted in the formation of a turbid mixture immediately, which is due to the efficient reaction and swelling of the DAC pulp in the AhG DES.(Selkälä et al., 2016; J. A. Sirviö, Visanko, et al., 2015)

The effects of different reaction temperatures and reaction times on the charge densities and yields of CDAC are presented in Figure 2. The results indicated that a high charge density, i.e., effective cationization, in the AhG DES was obtained when the reaction time was less than 15 min (Figure 2a and b). In a relative high temperature (>70°), the yield of CDAC55 started to decrease when the reaction time was longer than 15 min (Figure 2c), whereas the yield of CDAC75 became relatively stable after 30 min reaction (Figure 2d). However, in a mild temperature at 70°C, both CDAC55 and CDAC75 started to decrease their yield sharply after 30 min reaction. The increase in CDAC mass (yield > 100%) at low reaction times (<10 min) was due to the addition of large-molecular-weight cationic groups on cellulose during the reaction. In addition, DES residual might

attach to the CDAC could also lead to an unrealistic high yield. However, there was no direct relationship between the charge density and the yield, because the high charge density combined with elevated temperature and extended reaction time would also promote CDAC hydrolysis and dissolution, which in turn decreased the yield. For example, CDAC75 synthesized at 90°C and 30 min had a high charge density of 2.19 mmol g^{-1}, but a low yield of 50%. However, when the reaction temperature and time were decreased to 80°C and 10 min respectively, CDAC75 was obtained with a high charge density of 2.48 mmol g^{-1} along with a yield of 105%. Therefore, the yields reflect the combination effects of the introduced cationic groups, the degree of CDAC hydrolyzing and dissolution in DES and in ethanol during the washing, and the contribution of impurities (small amount of glycerol from DES can be attached to dialdehyde cellulose by acetal and hemiacetal formation).

Under the same DES reaction conditions, CDAC75 typically had higher charge densities than CDAC55. This result was due to the higher initial aldehyde content of its precursor compared to CDAC55.(J. Sirviö et al., 2011) In addition, there were clear trends for CDAC75, too: at all temperatures, the charge densities increased when the reaction time was increased from 5 to 10 min (Figure 2b). In the case of CDAC55, the charge density increased steadily at 70°C with prolonged reaction time. Moreover, there was no significant difference in charge densities in response to changes in temperature or reaction time (Figure 2a). Therefore, applying the AhG DES under mild conditions (reaction time of less than 15 min and temperatures of 70°C and 80°C) seems to be favorable for the production of cationized DAC with a high charge density and mass yield. Overall, compared with previous catalyst-assisted cationization or cationization reactions that required several hours,[75,76,87] AhG DES seems to be an effective solvent for the cationization

of aldehydes of cellulose. Further, from an up-scaling point of view, cationization through AhG DES could meet industrial needs on account of the low energy consumption and fast processing.

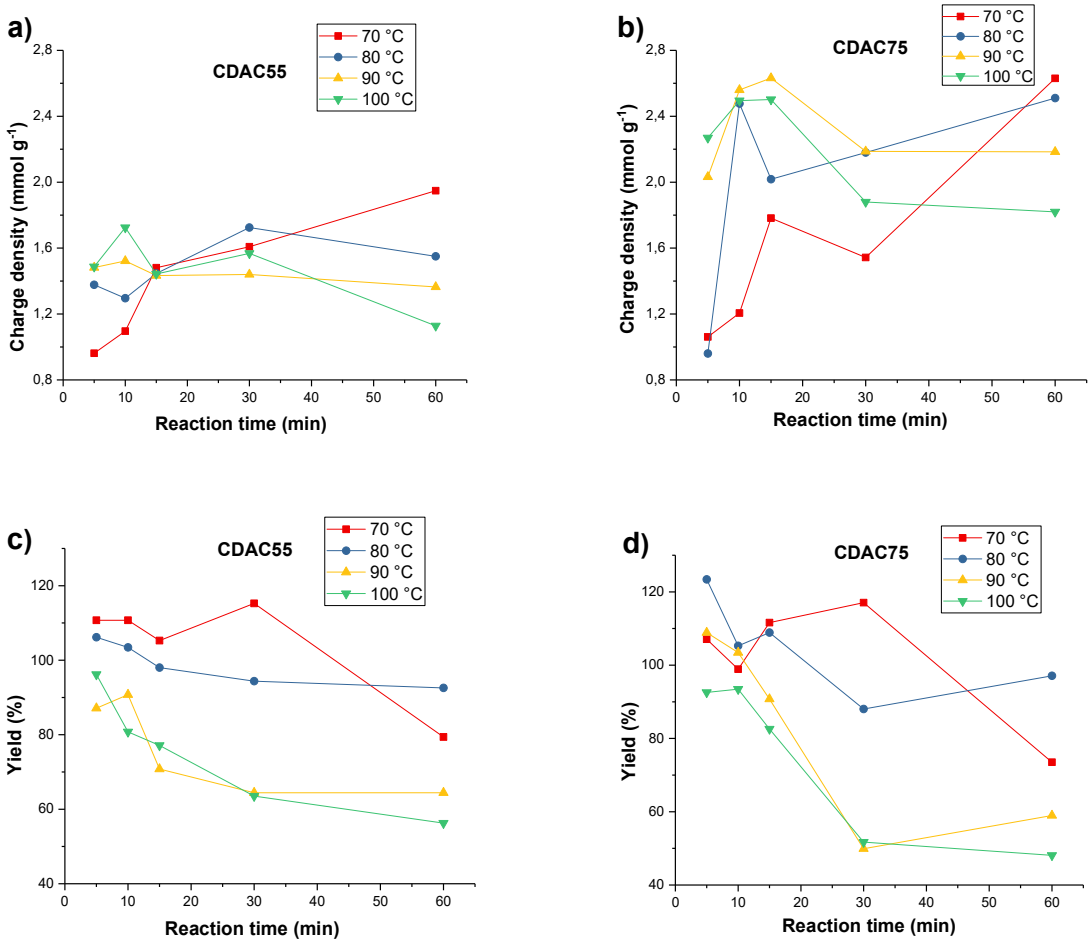

Figure 2. The charge density of CDAC55 (a) and CDAC75 (b), and the yield of CDAC55 (c) and CDAC75 (d), as a function of reaction time and temperature in cationization with AhG DES.

3.2 Characteristics of cationized celluloses

The original cellulose, DAC75 and AhG DES-synthesized CDAC75 (at 70°C for 10 min) were characterized by ATR-IR (Figure 3). The spectra of DAC75 and CDAC75 presented characteristic cellulosic bands in the range of 4000–2995 cm^{-1} that corresponded to OH stretching, an adsorption band at 2900 cm^{-1} that corresponded to CH stretching vibration, and a band at 1430 cm^{-1} that was

assigned to HCH and CHO in plane deformation vibrations.(Oh, Yoo, Shin, & Seo, 2005; J. A. Sirviö, Visanko, et al., 2015) The absorption band at 1728 cm^{-1}, which is characteristic of the aldehyde carbonyl group in DAC75, was replaced with new bands that appeared at 1674 cm^{-1} and 1635 cm^{-1} in CDAC75 and corresponded to the carbon-nitrogen double bond of imines and nitrogen-hydrogen bond bending, respectively. (J. A. Sirviö et al., 2014b; Y. Zhang, Jiang, & Chen, 1999). These findings indicated successful reaction between the aldehyde groups in DAC and aminoguanidine hydrochloride in the AhG DES.

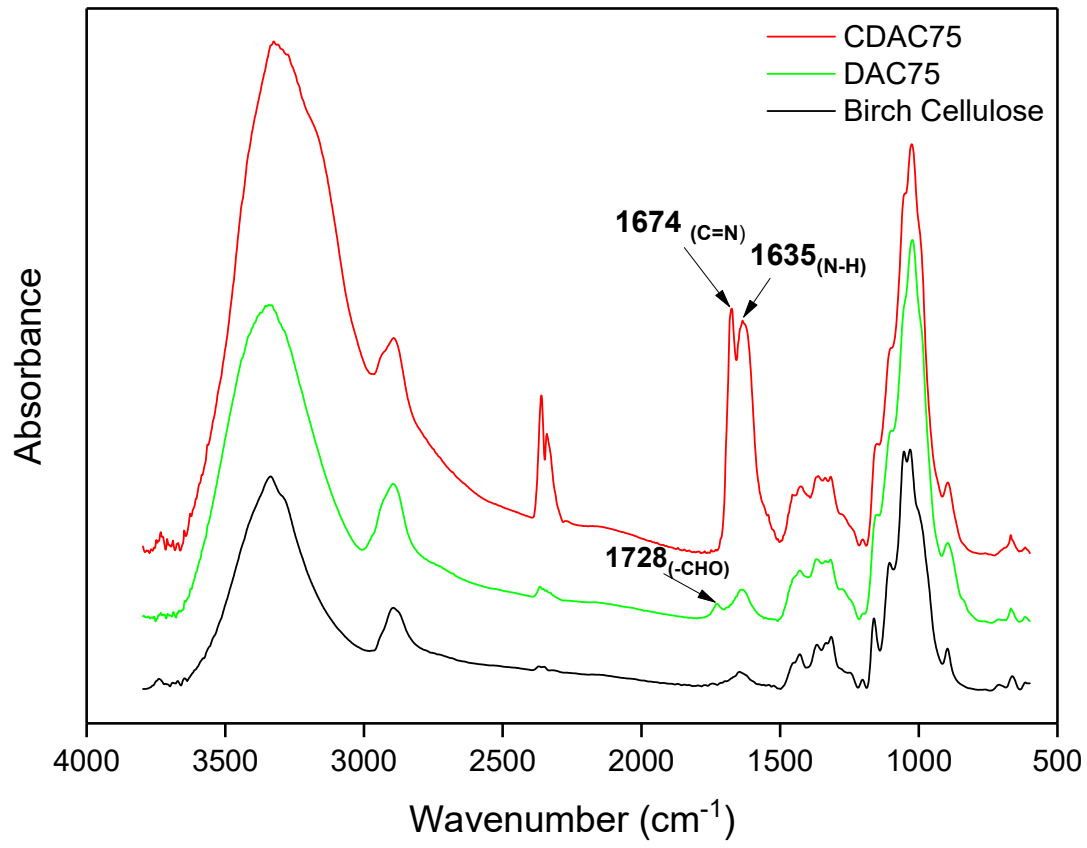

Figure 3. ATR-IR spectra of birch cellulose, DAC75 with the characteristic aldehyde band (1728 cm^{-1}), and CDAC75 with the characteristic carbon-nitrogen double bond (1674 cm^{-1}) and nitrogen-hydrogen bond (1635 cm^{-1}).

The reaction mechanisms of DAC cationization in the AhG DES can be explained in two ways: (1) The AhG DES enabled the aldehyde groups of DAC to form stable imine structures with aminoguanidine hydrochloride. The driving force of the reaction was the formation of the

conjugated imine structure.(Clayden, Greeves, & Warren, 2012) (2) The AhG DES worked simultaneously as a cellulose disintegrating medium by disrupting the internal and external hydrogen and hemiacetal/acetal bonds of DAC, which in turn enhanced the reaction efficiency and later promoted the mechanical disintegration process to lead to the production of functionalized nanocelluloses.(P. Li et al., 2017) In addition, the AhG DES could increase the reactivity of the aldehyde groups through formation of hydrogen bonds with carbonyl and thus increased the electrophilicity of the aldehyde carbon.(Guigo, Mazeau, Putaux, & Heux, 2014)

The XRD spectra of CDAC55 and CDAC75 (Figure 4) indicated an increase in crystallinity. I.e., after the DES cationization, the crystallinity of CDAC55 and CDAC75 were 63.2% and 64.9%, which were higher than the original birch pulp (56.6%) and previously reported to cationic cellulose synthesized in water (J. A. Sirviö et al., 2014b). These results suggested the dissolution of the amorphous parts of cellulose during AhG DES cationization.

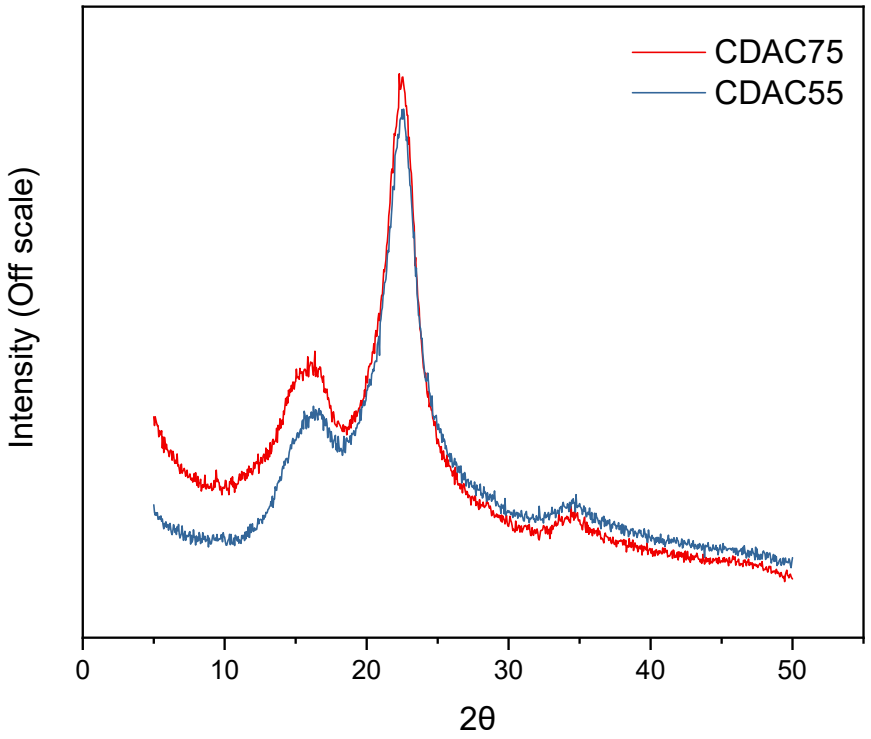

296

297 **Figure 4.** X-ray diffraction spectra of CDAC55 and CDAC75.

298

299 *3.3 Cationized nanocelluloses*

300 CDAC55 and CDAC75 treated with AhG DES at 70°C for 10 min were selected for
301 mechanical disintegration with a microfluidizer, owing to their relatively high charge density
302 (0.918 and 1.206 mmol g^{-1}, respectively). Unlike the raw cellulose and DAC fibers, there was no
303 chamber clogging(Carrillo, Laine, & Rojas, 2014; Siró & Plackett, 2010b) with the AhG-treated
304 CDAC55 and CDAC75. Both the samples smoothly passed through the microfluidizer chambers.
305 The introduced repulsive positive surface charges and the weakened hydrogen bonding network
306 of the cellulose fibers were useful for the mechanical disintegration. Furthermore, homogenous,
307 gel-like materials were obtained after the first pass through the microfluidizer, whereas the visual

difference was clearer when CDACs were passed through the chambers twice. This showed that the nanofibrillated CDAC55 was more turbid and viscous than the CDAC75 sample (Figure 5).

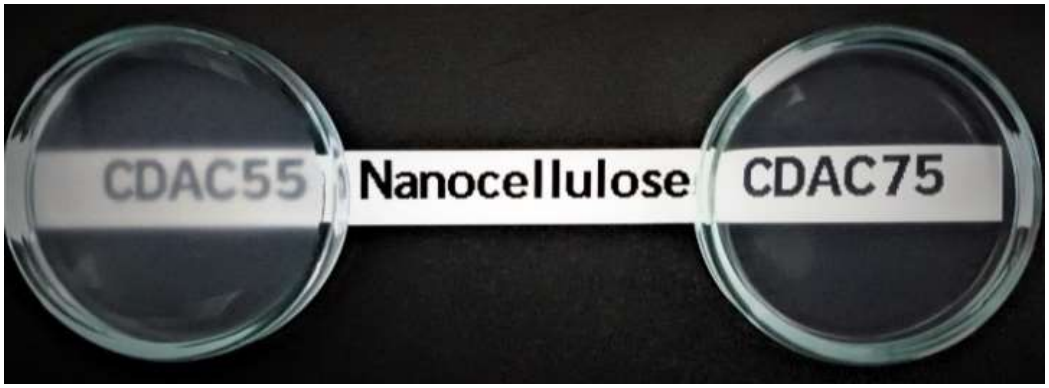

Figure 5. 1% CDAC55 (left) and CDAC75 (right) nanocellulose suspensions after mechanical disintegration.

The TEM images presented in Figure 6 confirm that both CDAC55 and CDAC75 formed nano-sized particles after mechanical disintegration; i.e., individual nanofibrils and nanocrystals with an average width of 4.6 ± 1.1 nm and 5.7 ± 1.3 nm were detected separately. Notably, CDAC75 generally consisted of shorter particles with a more rod-like structure that corresponded to cellulose nanocrystals,(Klemm et al., 2011) while CDAC55 mainly consisted of elongated and flexible nanofibrils. Therefore, the TEM images indicated that the morphology of nanocellulose could be tailored by the reaction conditions of AhG DES treatment, and that the nanofibrillation products of CDAC55 and CDAC75 were mainly CNFs and CNCs, respectively. The CNCs produced from AhG DES had a smaller width than previously reported with acidic DES (9−17 nm)(J. A. Sirviö, Visanko, & Liimatainen, 2016), while the CNFs had comparable width to those fabricated using DES-mediated succinylation (2−7 nm).(Selkälä et al., 2016) Besides, there were fewer but more dispersed web-like nanofibrous individual CNF or CNC structures observed from AhG DES-cationized nanocelluloses, which is different from the nanocelluloses obtained from urea-based DES pretreatment.(P. Li et al., 2017; J. A. Sirviö, Visanko, et al., 2015; Suopajärvi et al., 2017b) In addition to individual CNFs and CNCs, nanocellulose bundles (e.g., sequential periodate−chlorite oxidized nanofibrils with a width of 25 ± 6 nm(H. Liimatainen et al., 2012)) were rarely observed in both AhG DES-cationized nanocellulose samples; this finding is similar to that for nanocelluloses obtained from TEMPO-oxidization.(Habibi, Chanzy, & Vignon, 2006;

Saito, Kimura, Nishiyama, & Isogai, 2007) Overall, the AhG DES-cationized nanocelluloses had very similar behaviors to previously reported phosphonated nanocelluloses.(J. A. Sirviö, Hasa, et al., 2015) These findings indicate that according to the aldehyde content of DAC and charge density of CDAC, AhG DES combined with mechanical nanofibrillation led to the formation of cationic CNFs or CNCs. In the literature, periodate oxidation of cellulose is suggested to take place in clusters: that is, periodate molecules that are being formed preferentially react with the non-crystalline locations of celluloses near the previously oxidized regions.(Kim, Kuga, Wada, Okano, & Kondo, 2000; J. A. Sirviö, Hasa, et al., 2015) Therefore, the high degree of oxidation (DAC75) results in partial dissolution of the cellulose and breaking up of the fibers into short nanocrystals.

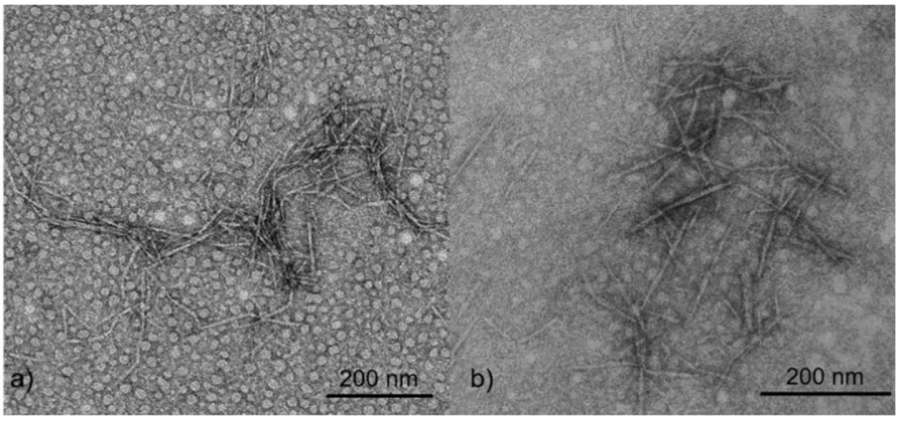

Figure 6. TEM images of nanofibrillated (a) CDAC55 and (b) CDAC75.

3.4 Recycling of AhG DES

Aminoguanidine hydrochloride started to precipitate in the original AhG DES at room temperature (Figure 7a). However, even after the reaction and recycling, the AhG DES formed a clear eutectic liquid at room temperature without any visible precipitation. This may be explained by the introduction of impurities, such as ethanol and water, which may promote the dissolution of aminoguanidine hydrochloride. The AhG DES maintained a clear liquid appearance after five reuses and became yellowish only gradually with the increase in heating cycles (Figure 7b–f). This

yellow color may originate from the impurities and degradation side products (e.g., cellulose and DES).(Guigo et al., 2014)

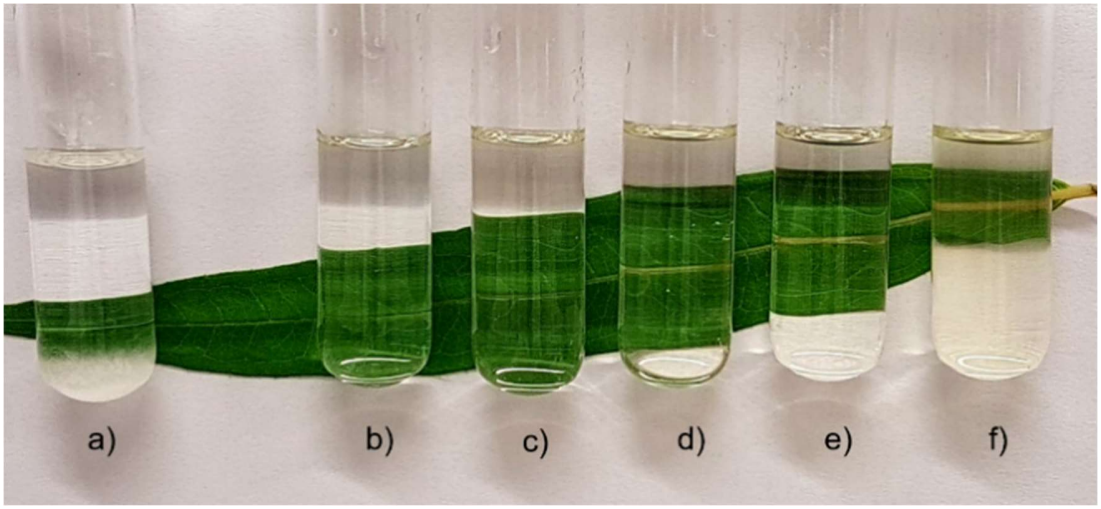

Figure 7. The original AhG DES (a), and recycled AhG DES (b–f) after one to five times of re-use at room temperature.

During the recycling of the AhG DES, the yield of DES was slightly reduced after prolonged recycling. The decrease in the yield may be a result of the consumption of aminoguanidine hydrochloride as a result of reaction with the aldehyde groups of DAC. Theoretically, 1.81% of aminoguanidine hydrochloride was consumed in a single reaction cycle. Therefore, there was clear decreased mass of DES can be seen after first cycle. However, in some cases, the chemical mass of recycled AhG DES was over 100%, which most likely was a result of the impurities (e.g., water and ethanol) that were tightly bonded and could not be fully removed by evaporation.(van Osch, Zubeir, van den Bruinhorst, Rocha, & Kroon, 2015) Although the introduction of water often affects the properties of DES (Du, Zhao, Chen, Birbilis, & Yang, 2016), the cationization reaction efficiency of AhG DES was not affected by impurities from the recycling procedure. As the polyelectrolyte titration results showed, both the original AhG DES and the recycled AhG DES were able to deliver DACs with the same level of cationic charge density after a 10-min reaction

at 70°C (Table 1), the charge densities of CDAC55 and CDAC75 being around 1 and 1.2 mmol g^{-1}, respectively. It was also noted that the charge density value increased after mechanical disintegration; that is, compared to their precursors, the charge density of nanocelluloses from CDAC55 and CDAC75 was 39% and 42% higher, respectively. It seems that some of the cationic groups inside the CDAC fibers became accessible to the large polymer PES-Na, which was used for polyelectrolyte titration after mechanical nanofibrillation (Table 1).

Table 1. Summary of the yield of recycled AhG DES and the yield and charge density of CDACs

Product	CDAC55			CDAC75		
Cycle	Yield of AhG DES (%)	Yield of CDAC55 (%)	Charge density (mmol g^{-1})	Yield of AhG DES (%)	Yield of CDAC75 (%)	Charge density (mmol g^{-1})
I	100±3.5	107±2.5	0.918	100±2.5	116±1.5	1.206
II	107±2.0	98±1.0	1.049	106±1.5	110±1.0	1.132
III	103±0.5	99±0.5	0.942	102±2.0	110±0.5	1.160
IV	100±1.5	98±0.5	1.026	96±2.5	108±1.5	1.180
V	99±0.5	93±2.0	1.021	93±0.5	96±3.5	1.221
Nano-fibrillation I			1.274			1.713

3.5 Thermal stability of AhG DES

Compared with previously reported glycerol-choline chloride DES (Delgado-Mellado et al., 2018), the original AhG DES showed similar results from thermogravimetric analysis (Figure 8). I.e., AhG DES had only one-step mass loss caused by the evaporation of glycerol and simultaneously thermal decomposition of aminoguanidine hydrochloride. It was also notable that

the onset decomposition temperature of AhG DES was much higher than the reaction temperature, which explains the reusability of AhG DES.

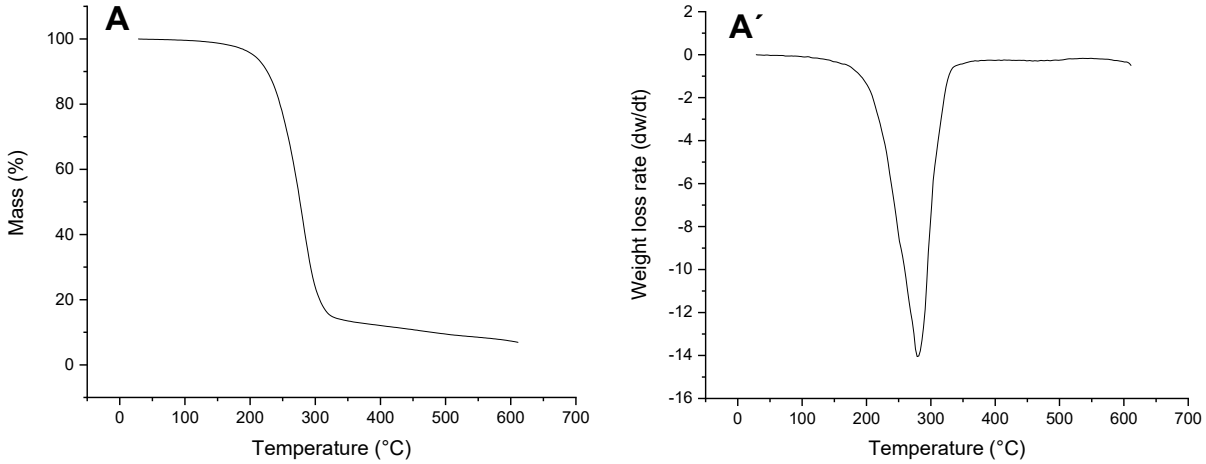

Figure 8. TGA and the first derivate of TGA of the original AhG DES at air condition.

4. Conclusion

The AhG DES formed by aminoguanidine hydrochloride and glycerol was found to be an effective and recyclable medium and reagent for the production of cationic celluloses from DAC under mild conditions (70°C for 10 min). The DES was reused five times by a simple distillation procedure, and the recycled DES exhibited similar reaction efficiency to the original DES. In addition, no additional chemicals were used during the recycling, which further improved the feasibility of using the AhG DES as a cationization medium. According to the initial aldehyde content of DACs, the cationized cellulose could be disintegrated to highly cationic CNFs or CNCs. Individual CNFs and CNCs had a width of around 5 nm, which indicates that this recyclable AhG DES presents an efficient and green option for functionalized nanocellulose production.

Acknowledgment

The study was supported by Safewood (Tekes and European Regional Development Fund: 3368/31/2015) and Bionanochemicals (Academy of Finland Grant: 298295) Projects.

REFERENCES

Abbott, A. P., Cullis, P. M., Gibson, M. J., Harris, R. C., & Raven, E. (2007). Extraction of glycerol from biodiesel into a eutectic based ionic liquid. *Green Chemistry*, *9*(8), 868. https://doi.org/10.1039/b702833d

Abbott, A. P., Harris, R. C., Ryder, K. S., D'Agostino, C., Gladden, L. F., & Mantle, M. D. (2011). Glycerol eutectics as sustainable solvent systems. *Green Chem.*, *13*(1), 82–90. https://doi.org/10.1039/C0GC00395F

Alonso, D. A., Baeza, A., Chinchilla, R., Guillena, G., Pastor, I. M., & Ramón, D. J. (2016). Deep Eutectic Solvents: The Organic Reaction Medium of the Century. *European Journal of Organic Chemistry*, *2016*(4), 612–632. https://doi.org/10.1002/ejoc.201501197

Araki, J., Wada, M., Kuga, S., & Okano, T. (1998). Flow properties of microcrystalline cellulose suspension prepared by acid treatment of native cellulose. *Colloids and Surfaces A: Physicochemical and Engineering Aspects*, *142*(1), 75–82. Retrieved from http://www.sciencedirect.com/science/article/pii/S092777579800404X

Baati, R., Magnin, A., & Boufi, S. (2017). High Solid Content Production of Nanofibrillar Cellulose via Continuous Extrusion. *ACS Sustainable Chemistry & Engineering*, *5*(3), 2350–2359. https://doi.org/10.1021/acssuschemeng.6b02673

417 Bondeson, D., Mathew, A., & Oksman, K. (2006). Optimization of the isolation of nanocrystals
418 from microcrystalline cellulose by acid hydrolysis. *Cellulose*, *13*(2), 171–180.
419 https://doi.org/10.1007/s10570-006-9061-4
420 Camarero Espinosa, S., Kuhnt, T., Foster, E. J., & Weder, C. (2013). Isolation of Thermally Stable
421 Cellulose Nanocrystals by Phosphoric Acid Hydrolysis. *Biomacromolecules*, *14*(4), 1223–
422 1230. https://doi.org/10.1021/bm400219u
423 Carrillo, C. A., Laine, J., & Rojas, O. J. (2014). Microemulsion Systems for Fiber Deconstruction
424 into Cellulose Nanofibrils. *ACS Applied Materials & Interfaces*, *6*(24), 22622–22627.
425 https://doi.org/10.1021/am5067332
426 Clayden, J., Greeves, N., & Warren, S. (2012). *Organic Chemistry*. OUP Oxford.
427 Corrêa, A. C., de Morais Teixeira, E., Pessan, L. A., & Mattoso, L. H. C. (2010). Cellulose
428 nanofibers from curaua fibers. *Cellulose*, *17*(6), 1183–1192.
429 https://doi.org/10.1007/s10570-010-9453-3
430 Cravotto, G., Orio, L., Gaudino, E. C., Martina, K., Tavor, D., & Wolfson, A. (2011). Efficient
431 Synthetic Protocols in Glycerol under Heterogeneous Catalysis. *ChemSusChem*, *4*(8),
432 1130–1134. https://doi.org/10.1002/cssc.201100106
433 Credou, J., & Berthelot, T. (2014). Cellulose: from biocompatible to bioactive material. *J. Mater.*
434 *Chem. B*, *2*(30), 4767–4788. https://doi.org/10.1039/C4TB00431K
435 Cruz, H., Jordão, N., & Branco, L. C. (2017). Deep eutectic solvents (DESs) as low-cost and green
436 electrolytes for electrochromic devices. *Green Chem.*, *19*(7), 1653–1658.
437 https://doi.org/10.1039/C7GC00347A

438 Dash, R., Elder, T., & Ragauskas, A. J. (2012). Grafting of model primary amine compounds to
439 cellulose nanowhiskers through periodate oxidation. *Cellulose*, *19*(6), 2069–2079.
440 https://doi.org/10.1007/s10570-012-9769-2
441 Delgado-Mellado, N., Larriba, M., Navarro, P., Rigual, V., Ayuso, M., García, J., & Rodríguez,
442 F. (2018). Thermal stability of choline chloride deep eutectic solvents by TGA/FTIR-ATR
443 analysis. *Journal of Molecular Liquids*, *260*, 37–43.
444 https://doi.org/10.1016/j.molliq.2018.03.076
445 Díaz-Álvarez, A. E., Crochet, P., & Cadierno, V. (2011). Ruthenium-catalyzed reduction of allylic
446 alcohols using glycerol as solvent and hydrogen donor. *Catalysis Communications*, *13*(1),
447 91–96. https://doi.org/10.1016/j.catcom.2011.07.006
448 Du, C., Zhao, B., Chen, X.-B., Birbilis, N., & Yang, H. (2016). Effect of water presence on choline
449 chloride-2urea ionic liquid and coating platings from the hydrated ionic liquid. *Scientific*
450 *Reports*, *6*(1). https://doi.org/10.1038/srep29225
451 Eyley, S., & Thielemans, W. (2011). Imidazolium grafted cellulose nanocrystals for ion exchange
452 applications. *Chemical Communications*, *47*(14), 4177.
453 https://doi.org/10.1039/c0cc05359g
454 García, J. I., García-Marín, H., & Pires, E. (2014). Glycerol based solvents: synthesis, properties
455 and applications. *Green Chem.*, *16*(3), 1007–1033. https://doi.org/10.1039/C3GC41857J
456 Gu, Y., & Jérôme, F. (2010). Glycerol as a sustainable solvent for green chemistry. *Green*
457 *Chemistry*, *12*(7), 1127. https://doi.org/10.1039/c001628d
458 Guigo, N., Mazeau, K., Putaux, J.-L., & Heux, L. (2014). Surface modification of cellulose
459 microfibrils by periodate oxidation and subsequent reductive amination with benzylamine:

460 a topochemical study. *Cellulose*, *21*(6), 4119–4133. https://doi.org/10.1007/s10570-014-
461 0459-0
462 Habibi, Y., Chanzy, H., & Vignon, M. R. (2006). TEMPO-mediated surface oxidation of cellulose
463 whiskers. *Cellulose*, *13*(6), 679–687. https://doi.org/10.1007/s10570-006-9075-y
464 Hasani, M., Cranston, E. D., Westman, G., & Gray, D. G. (2008). Cationic surface
465 functionalization of cellulose nanocrystals. *Soft Matter*, *4*(11), 2238–2244.
466 https://doi.org/10.1039/B806789A
467 Henriksson, M., Henriksson, G., Berglund, L. A., & Lindström, T. (2007). An environmentally
468 friendly method for enzyme-assisted preparation of microfibrillated cellulose (MFC)
469 nanofibers. *European Polymer Journal*, *43*(8), 3434–3441.
470 https://doi.org/10.1016/j.eurpolymj.2007.05.038
471 Hernáiz, M. J., Alcántara, A. R., García, J. I., & Sinisterra, J. V. (2010). Applied
472 Biotransformations in Green Solvents. *Chemistry – A European Journal*, *16*(31), 9422–
473 9437. https://doi.org/10.1002/chem.201000798
474 Hua, K., Carlsson, D. O., Ålander, E., Lindström, T., Strømme, M., Mihranyan, A., & Ferraz, N.
475 (2014). Translational study between structure and biological response of nanocellulose
476 from wood and green algae. *RSC Adv.*, *4*(6), 2892–2903.
477 https://doi.org/10.1039/C3RA45553J
478 Ilgen, F., Ott, D., Kralisch, D., Reil, C., Palmberger, A., & König, B. (2009). Conversion of
479 carbohydrates into 5-hydroxymethylfurfural in highly concentrated low melting mixtures.
480 *Green Chemistry*, *11*(12), 1948. https://doi.org/10.1039/b917548m

Imperato, G., König, B., & Chiappe, C. (2007). Ionic Green Solvents from Renewable Resources. *European Journal of Organic Chemistry*, *2007*(7), 1049–1058. https://doi.org/10.1002/ejoc.200600435

Jasmani, L., Eyley, S., Wallbridge, R., & Thielemans, W. (2013). A facile one-pot route to cationic cellulose nanocrystals. *Nanoscale*, *5*(21), 10207. https://doi.org/10.1039/c3nr03456a

Jin, L., Li, W., Xu, Q., & Sun, Q. (2015). Amino-functionalized nanocrystalline cellulose as an adsorbent for anionic dyes. *Cellulose*, *22*(4), 2443–2456. https://doi.org/10.1007/s10570-015-0649-4

Kenawy, I. M., Hafez, M. A. H., Ismail, M. A., & Hashem, M. A. (2017). Adsorption of Cu(II), Cd(II), Hg(II), Pb(II) and Zn(II) from aqueous single metal solutions by guanyl-modified cellulose. *International Journal of Biological Macromolecules*. https://doi.org/10.1016/j.ijbiomac.2017.10.017

Khaksar, S. (2015). Fluorinated alcohols: A magic medium for the synthesis of heterocyclic compounds. *Journal of Fluorine Chemistry*, *172*, 51–61. https://doi.org/10.1016/j.jfluchem.2015.01.008

Kim, U.-J., Kuga, S., Wada, M., Okano, T., & Kondo, T. (2000). Periodate Oxidation of Crystalline Cellulose. *Biomacromolecules*, *1*(3), 488–492. https://doi.org/10.1021/bm0000337

Klemm, D., Kramer, F., Moritz, S., Lindström, T., Ankerfors, M., Gray, D., & Dorris, A. (2011). Nanocelluloses: A New Family of Nature-Based Materials. *Angewandte Chemie International Edition*, *50*(24), 5438–5466. https://doi.org/10.1002/anie.201001273

Kong, P. S., Aroua, M. K., Daud, W. M. A. W., Lee, H. V., Cognet, P., & Pérès, Y. (2016). Catalytic role of solid acid catalysts in glycerol acetylation for the production of bio-additives: a review. *RSC Adv.*, *6*(73), 68885–68905. https://doi.org/10.1039/C6RA10686B

Laitinen, O., Hartmann, R., Sirviö, J. A., Liimatainen, H., Rudolph, M., Ämmälä, A., & Illikainen, M. (2016). Alkyl aminated nanocelluloses in selective flotation of aluminium oxide and quartz. *Chemical Engineering Science*, *144*, 260–266. https://doi.org/10.1016/j.ces.2016.01.052

Laitinen, Ossi, Kemppainen, K., Ämmälä, A., Sirviö, J. A., Liimatainen, H., & Niinimäki, J. (2014). Use of Chemically Modified Nanocelluloses in Flotation of Hematite and Quartz. *Industrial & Engineering Chemistry Research*, *53*(52), 20092–20098. https://doi.org/10.1021/ie503415t

Laitinen, Ossi, Ojala, J., Sirviö, J. A., & Liimatainen, H. (2017). Sustainable stabilization of oil in water emulsions by cellulose nanocrystals synthesized from deep eutectic solvents. *Cellulose*, *24*(4), 1679–1689. https://doi.org/10.1007/s10570-017-1226-9

Laitinen, Ossi, Suopajärvi, T., Österberg, M., & Liimatainen, H. (2017). Hydrophobic, Superabsorbing Aerogels from Choline Chloride-Based Deep Eutectic Solvent Pretreated and Silylated Cellulose Nanofibrils for Selective Oil Removal. *ACS Applied Materials & Interfaces*, *9*(29), 25029–25037. https://doi.org/10.1021/acsami.7b06304

Leung, A. C. W., Hrapovic, S., Lam, E., Liu, Y., Male, K. B., Mahmoud, K. A., & Luong, J. H. T. (2011). Characteristics and Properties of Carboxylated Cellulose Nanocrystals Prepared from a Novel One-Step Procedure. *Small*, *7*(3), 302–305. https://doi.org/10.1002/smll.201001715

524 Li, C.-J., & Chen, L. (2006). Organic chemistry in water. *Chem. Soc. Rev.*, *35*(1), 68–82.
525 https://doi.org/10.1039/B507207G
526 Li, P., Sirviö, J. A., Haapala, A., & Liimatainen, H. (2017). Cellulose Nanofibrils from
527 Nonderivatizing Urea-Based Deep Eutectic Solvent Pretreatments. *ACS Applied Materials*
528 *& Interfaces*, *9*(3), 2846–2855. https://doi.org/10.1021/acsami.6b13625
529 Liimatainen, H., Visanko, M., Sirviö, J. A., Hormi, O. E. O., & Niinimaki, J. (2012). Enhancement
530 of the nanofibrillation of wood cellulose through sequential periodate-chlorite oxidation.
531 *Biomacromolecules*, *13*(5), 1592–1597. https://doi.org/10.1021/bm300319m
532 Liimatainen, Henrikki, Sirviö, J., Haapala, A., Hormi, O., & Niinimäki, J. (2011). Characterization
533 of highly accessible cellulose microfibers generated by wet stirred media milling.
534 *Carbohydrate Polymers*, *83*(4), 2005–2010. https://doi.org/10.1016/j.carbpol.2010.11.007
535 Liimatainen, Henrikki, Sirviö, J., Pajari, H., Hormi, O., & Niinimäki, J. (2013). Regeneration and
536 Recycling of Aqueous Periodate Solution in Dialdehyde Cellulose Production. *Journal of*
537 *Wood Chemistry and Technology*, *33*(4), 258–266.
538 https://doi.org/10.1080/02773813.2013.783076
539 Liimatainen, Henrikki, Suopajärvi, T., Sirviö, J., Hormi, O., & Niinimäki, J. (2014). Fabrication
540 of cationic cellulosic nanofibrils through aqueous quaternization pretreatment and their use
541 in colloid aggregation. *Carbohydrate Polymers*, *103*, 187–192.
542 https://doi.org/10.1016/j.carbpol.2013.12.042
543 Lu, Q., Cai, Z., Lin, F., Tang, L., Wang, S., & Huang, B. (2016). Extraction of Cellulose
544 Nanocrystals with a High Yield of 88% by Simultaneous Mechanochemical Activation and
545 Phosphotungstic Acid Hydrolysis. *ACS Sustainable Chemistry & Engineering*, *4*(4), 2165–
546 2172. https://doi.org/10.1021/acssuschemeng.5b01620

547 Marsich, L., Bonifacio, A., Mandal, S., Krol, S., Beleites, C., & Sergo, V. (2012). Poly-l-lysine-
548 Coated Silver Nanoparticles as Positively Charged Substrates for Surface-Enhanced
549 Raman Scattering. *Langmuir*, *28*(37), 13166–13171. https://doi.org/10.1021/la302383r
550 Mohieldin, S. D., Zainudin, E. S., Paridah, M. T., & Ainun, Z. M. (2011). Nanotechnology in Pulp
551 and Paper Industries: A Review. *Key Engineering Materials*, *471–472*, 251–256.
552 https://doi.org/10.4028/www.scientific.net/KEM.471-472.251
553 Montanari, S., Roumani, M., Heux, L., & Vignon, M. R. (2005). Topochemistry of Carboxylated
554 Cellulose Nanocrystals Resulting from TEMPO-Mediated Oxidation. *Macromolecules*,
555 *38*(5), 1665–1671. https://doi.org/10.1021/ma048396c
556 Moon, R. J., Martini, A., Nairn, J., Simonsen, J., & Youngblood, J. (2011). Cellulose
557 nanomaterials review: structure, properties and nanocomposites. *Chemical Society*
558 *Reviews*, *40*(7), 3941. https://doi.org/10.1039/c0cs00108b
559 Oh, S. Y., Yoo, D. I., Shin, Y., & Seo, G. (2005). FTIR analysis of cellulose treated with sodium
560 hydroxide and carbon dioxide. *Carbohydrate Research*, *340*(3), 417–428.
561 https://doi.org/10.1016/j.carres.2004.11.027
562 Ojala, J., Sirviö, J. A., & Liimatainen, H. (2016). Nanoparticle emulsifiers based on
563 bifunctionalized cellulose nanocrystals as marine diesel oil–water emulsion stabilizers.
564 *Chemical Engineering Journal*, *288*, 312–320. https://doi.org/10.1016/j.cej.2015.10.113
565 Oksman, K., Mathew, A. P., Bondeson, D., & Kvien, I. (2006). Manufacturing process of cellulose
566 whiskers/polylactic acid nanocomposites. *Composites Science and Technology*, *66*(15),
567 2776–2784. https://doi.org/10.1016/j.compscitech.2006.03.002

568 Paiva, A., Craveiro, R., Aroso, I., Martins, M., Reis, R. L., & Duarte, A. R. C. (2014). Natural
569 Deep Eutectic Solvents – Solvents for the 21st Century. *ACS Sustainable Chemistry &*
570 *Engineering*, *2*(5), 1063–1071. https://doi.org/10.1021/sc500096j
571 Qin, Z.-Y., Tong, G., Chin, Y. C. F., & Zhou, J.-C. (2011). PREPARATION OF ULTRASONIC-
572 ASSISTED HIGH CARBOXYLATE CONTENT CELLULOSE NANOCRYSTALS BY
573 TEMPO OXIDATION. *BioResources*, *6*(2), 1136–1146.
574 https://doi.org/10.15376/biores.6.2.1136-1146
575 Saito, T., Kimura, S., Nishiyama, Y., & Isogai, A. (2007). Cellulose nanofibers prepared by
576 TEMPO-mediated oxidation of native cellulose. *Biomacromolecules*, *8*(8), 2485–2491.
577 https://doi.org/10.1021/bm0703970
578 Saito, T., Nishiyama, Y., Putaux, J.-L., Vignon, M., & Isogai, A. (2006). Homogeneous
579 Suspensions of Individualized Microfibrils from TEMPO-Catalyzed Oxidation of Native
580 Cellulose. *Biomacromolecules*, *7*(6), 1687–1691. https://doi.org/10.1021/bm060154s
581 Schenzel, A., Hufendiek, A., Barner-Kowollik, C., & Meier, M. A. R. (2014). Catalytic
582 transesterification of cellulose in ionic liquids: sustainable access to cellulose esters. *Green*
583 *Chemistry*, *16*(6), 3266. https://doi.org/10.1039/c4gc00312h
584 Segal, L., Creely, J. J., A. E. Martin, J., & Conrad, C. M. (2016). An Empirical Method for
585 Estimating the Degree of Crystallinity of Native Cellulose Using the X-Ray
586 Diffractometer: *Textile Research Journal*. https://doi.org/10.1177/004051755902901003
587 Selkälä, T., Sirviö, J. A., Lorite, G. S., & Liimatainen, H. (2016). Anionically Stabilized Cellulose
588 Nanofibrils through Succinylation Pretreatment in Urea-Lithium Chloride Deep Eutectic
589 Solvent. *ChemSusChem*. https://doi.org/10.1002/cssc.201600903

590 Shahid, M., Mohammad, F., Chen, G., Tang, R.-C., & Xing, T. (2016). Enzymatic processing of
591 natural fibres: white biotechnology for sustainable development. *Green Chem.*, *18*(8),
592 2256–2281. https://doi.org/10.1039/C6GC00201C
593 Singh, B., Lobo, H., & Shankarling, G. (2011). Selective N-Alkylation of Aromatic Primary
594 Amines Catalyzed by Bio-catalyst or Deep Eutectic Solvent. *Catalysis Letters*, *141*(1),
595 178–182. https://doi.org/10.1007/s10562-010-0479-9
596 Siró, I., & Plackett, D. (2010a). Microfibrillated cellulose and new nanocomposite materials: a
597 review. *Cellulose*, *17*(3), 459–494. https://doi.org/10.1007/s10570-010-9405-y
598 Siró, I., & Plackett, D. (2010b). Microfibrillated cellulose and new nanocomposite materials: a
599 review. *Cellulose*, *17*(3), 459–494. https://doi.org/10.1007/s10570-010-9405-y
600 Sirviö, J. A. (n.d.). Cationization of lignocellulosic fibers with betaine in deep eutectic solvent:
601 facile route to charge stabilized cellulose and wood nanofibers. *Carbohydrate Polymers*.
602 https://doi.org/10.1016/j.carbpol.2018.06.051
603 Sirviö, J. A., Anttila, A.-K., Pirttilä, A. M., Liimatainen, H., Kilpeläinen, I., Niinimäki, J., &
604 Hormi, O. (2014a). Cationic wood cellulose films with high strength and bacterial anti-
605 adhesive properties. *Cellulose*, *21*(5), 3573–3583. https://doi.org/10.1007/s10570-014-
606 0351-y
607 Sirviö, J. A., Anttila, A.-K., Pirttilä, A. M., Liimatainen, H., Kilpeläinen, I., Niinimäki, J., &
608 Hormi, O. (2014b). Cationic wood cellulose films with high strength and bacterial anti-
609 adhesive properties. *Cellulose*, *21*(5), 3573–3583. https://doi.org/10.1007/s10570-014-
610 0351-y
611 Sirviö, J. A., Hasa, T., Ahola, J., Liimatainen, H., Niinimäki, J., & Hormi, O. (2015). Phosphonated
612 nanocelluloses from sequential oxidative–reductive treatment—Physicochemical

613 characteristics and thermal properties. *Carbohydrate Polymers*, *133*, 524–532.
614 https://doi.org/10.1016/j.carbpol.2015.06.090
615 Sirviö, J. A., Visanko, M., Heiskanen, J. P., & Liimatainen, H. (2016). UV-absorbing cellulose
616 nanocrystals as functional reinforcing fillers in polymer nanocomposite films. *J. Mater.*
617 *Chem. A*, *4*(17), 6368–6375. https://doi.org/10.1039/C6TA00900J
618 Sirviö, J. A., Visanko, M., & Liimatainen, H. (2015). Deep eutectic solvent system based on
619 choline chloride-urea as a pre-treatment for nanofibrillation of wood cellulose. *Green*
620 *Chemistry*, *17*(6), 3401–3406. Retrieved from
621 http://pubs.rsc.org/is/content/articlehtml/2015/gc/c5gc00398a
622 Sirviö, J. A., Visanko, M., & Liimatainen, H. (2016). Acidic Deep Eutectic Solvents As Hydrolytic
623 Media for Cellulose Nanocrystal Production. *Biomacromolecules*, *17*(9), 3025–3032.
624 https://doi.org/10.1021/acs.biomac.6b00910
625 Sirviö, J. A., & Visanko, M. T. (2017). Anionic wood nanofibers produced from unbleached
626 mechanical pulp by highly efficient chemical modification. *J. Mater. Chem. A*.
627 https://doi.org/10.1039/C7TA05668K
628 Sirviö, J. A., Visanko, M., Ukkola, J., & Liimatainen, H. (2018). Effect of plasticizers on the
629 mechanical and thermomechanical properties of cellulose-based biocomposite films.
630 *Industrial Crops and Products*, *122*, 513–521.
631 https://doi.org/10.1016/j.indcrop.2018.06.039
632 Sirviö, J., Honka, A., Liimatainen, H., Niinimäki, J., & Hormi, O. (2011). Synthesis of highly
633 cationic water-soluble cellulose derivative and its potential as novel biopolymeric
634 flocculation agent. *Carbohydrate Polymers*, *86*(1), 266–270.
635 https://doi.org/10.1016/j.carbpol.2011.04.046

636 Sirvio, J., Hyvakko, U., Liimatainen, H., Niinimaki, J., & Hormi, O. (2011). Periodate oxidation
637 of cellulose at elevated temperatures using metal salts as cellulose activators. *Carbohydrate*
638 *Polymers*, *83*(3), 1293–1297. Retrieved from
639 http://www.sciencedirect.com/science/article/pii/S0144861710007691
640 Smith, E. L., Abbott, A. P., & Ryder, K. S. (2014). Deep Eutectic Solvents (DESs) and Their
641 Applications. *Chemical Reviews*, *114*(21), 11060–11082.
642 https://doi.org/10.1021/cr300162p
643 Suopajärvi, T., Sirviö, J. A., & Liimatainen, H. (2017a). Cationic nanocelluloses in dewatering of
644 municipal activated sludge. *Journal of Environmental Chemical Engineering*, *5*(1), 86–92.
645 https://doi.org/10.1016/j.jece.2016.11.021
646 Suopajärvi, T., Sirviö, J. A., & Liimatainen, H. (2017b). Nanofibrillation of deep eutectic solvent-
647 treated paper and board cellulose pulps. *Carbohydrate Polymers*, *169*, 167–175.
648 https://doi.org/10.1016/j.carbpol.2017.04.009
649 van Osch, D. J. G. P., Zubeir, L. F., van den Bruinhorst, A., Rocha, M. A. A., & Kroon, M. C.
650 (2015). Hydrophobic deep eutectic solvents as water-immiscible extractants. *Green Chem.*,
651 *17*(9), 4518–4521. https://doi.org/10.1039/C5GC01451D
652 Visanko, M., Liimatainen, H., Sirviö, J. A., Heiskanen, J. P., Niinimäki, J., & Hormi, O. (2014).
653 Amphiphilic Cellulose Nanocrystals from Acid-Free Oxidative Treatment:
654 Physicochemical Characteristics and Use as an Oil–Water Stabilizer. *Biomacromolecules*,
655 *15*(7), 2769–2775. https://doi.org/10.1021/bm500628g
656 Wagle, D. V., Zhao, H., & Baker, G. A. (2014). Deep Eutectic Solvents: Sustainable Media for
657 Nanoscale and Functional Materials. *Accounts of Chemical Research*, *47*(8), 2299–2308.
658 https://doi.org/10.1021/ar5000488

659 Wang, Y., Hou, Y., Wu, W., Liu, D., Ji, Y., & Ren, S. (2016). Roles of a hydrogen bond donor
660 and a hydrogen bond acceptor in the extraction of toluene from n-heptane using deep
661 eutectic solvents. *Green Chem.*, *18*(10), 3089–3097. https://doi.org/10.1039/C5GC02909K
662 Wolfson, A., Dlugy, C., & Shotland, Y. (2007). Glycerol as a green solvent for high product yields
663 and selectivities. *Environmental Chemistry Letters*, *5*(2), 67–71.
664 https://doi.org/10.1007/s10311-006-0080-z
665 Wolfson, A., Dlugy, C., Tavor, D., Blumenfeld, J., & Shotland, Y. (2006). Baker's yeast catalyzed
666 asymmetric reduction in glycerol. *Tetrahedron: Asymmetry*, *17*(14), 2043–2045.
667 https://doi.org/10.1016/j.tetasy.2006.07.026
668 Yang, H., & van de Ven, T. G. M. (2016). Preparation of hairy cationic nanocrystalline cellulose.
669 *Cellulose*, *23*(3), 1791–1801. https://doi.org/10.1007/s10570-016-0902-5
670 Yu, H., Qin, Z., Liang, B., Liu, N., Zhou, Z., & Chen, L. (2013). Facile extraction of thermally
671 stable cellulose nanocrystals with a high yield of 93% through hydrochloric acid hydrolysis
672 under hydrothermal conditions. *Journal of Materials Chemistry A*, *1*(12), 3938.
673 https://doi.org/10.1039/c3ta01150j
674 Zhang, J., Jiang, N., Dang, Z., Elder, T. J., & Ragauskas, A. J. (2008). Oxidation and sulfonation
675 of cellulosics. *Cellulose*, *15*(3), 489–496. https://doi.org/10.1007/s10570-007-9193-1
676 Zhang, K., Sun, P., Liu, H., Shang, S., Song, J., & Wang, D. (2016). Extraction and comparison
677 of carboxylated cellulose nanocrystals from bleached sugarcane bagasse pulp using two
678 different oxidation methods. *Carbohydrate Polymers*, *138*, 237–243.
679 https://doi.org/10.1016/j.carbpol.2015.11.038

Zhang, Q., De Oliveira Vigier, K., Royer, S., & Jérôme, F. (2012). Deep eutectic solvents: syntheses, properties and applications. *Chemical Society Reviews*, *41*(21), 7108. https://doi.org/10.1039/c2cs35178a

Zhang, W., Barone, J. R., & Renneckar, S. (2015). Biomass Fractionation after Denaturing Cell Walls by Glycerol Thermal Processing. *ACS Sustainable Chemistry & Engineering*, *3*(3), 413–420. https://doi.org/10.1021/sc500564g

Zhang, Y., Jiang, J., & Chen, Y. (1999). Synthesis and antimicrobial activity of polymeric guanidine and biguanidine salts. *Polymer*, *40*(22), 6189–6198. Retrieved from http://www.sciencedirect.com/science/article/pii/S0032386198008283

Zhao, H., & Baker, G. A. (2013). Ionic liquids and deep eutectic solvents for biodiesel synthesis: a review. *Journal of Chemical Technology & Biotechnology*, *88*(1), 3–12. https://doi.org/10.1002/jctb.3935

Zhou, Y., Khan, T. M., Liu, J.-C., Fuentes-Hernandez, C., Shim, J. W., Najafabadi, E., … Kippelen, B. (2014). Efficient recyclable organic solar cells on cellulose nanocrystal substrates with a conducting polymer top electrode deposited by film-transfer lamination. *Organic Electronics*, *15*(3), 661–666. https://doi.org/10.1016/j.orgel.2013.12.018